Quantal Basis of Photoreceptor Spectral Sensitivity of *Drosophila melanogaster*

CHUN-FANG WU and WILLIAM L. PAK

From the Department of Biological Sciences, Purdue University, West Lafayette, Indiana 47907

ABSTRACT Small potential fluctuations ("bumps"), both spontaneous and light induced, can be recorded intracellularly from the photoreceptors of *Drosophila melanogaster*. Statistical analyses of these bumps in the spectral range, 400–600 nm, lead to the following interpretations; (*a*) For weak stimuli at least, these bumps are the quantal units of the receptor potential. (*b*) Quanta of various wavelengths, when effectively absorbed, will elicit bumps of the same average size. (*c*) The spectral sensitivity of the receptor potential appears to have its origin in the relative efficiency of quantum bump production at different wavelengths, and not in the intrinsic difference in the properties of bumps produced by quanta of different wavelengths.

INTRODUCTION

Small discrete voltage fluctuations, commonly called "bumps," can be recorded intracellularly both in the dark (spontaneous bumps) and in dim light (light-induced bumps) from the photoreceptor cells of several species of arthropods (*Limulus* lateral eyes: Yeandle, 1957; Fuortes and Yeandle, 1964; Adolph, 1964; *Limulus* ventral eyes: Millecchia and Mauro, 1969; *Locusta:* Scholes, 1965; and *Musca:* Kirschfeld, 1966). The rate of occurrence of the bumps increases in proportion to light intensity, but the time of occurrence appears to be random and independent (Fuortes and Yeandle, 1964; Adolph, 1964; Scholes, 1965). The frequency distribution of bumps elicited by brief flashes suggests that a light-induced bump is triggered by absorption of a single photon (Fuortes and Yeandle, 1964; Scholes, 1965; Borsellino and Fuortes, 1968). Moreover, the shot noise analysis of Dodge et al. (1968) provided evidence that the generator potential of the photoreceptor cell is simply a summation of these bumps. Some critical questions, however, remain unanswered. (*a*) How are spontaneous and light-induced bumps related to each other? (*b*) Does the principle of univariance (Rushton, 1972) hold at the quantum bump level? In other words, is each photon absorbed by visual pigment equivalent in eliciting a quantum bump regardless of its wavelength?

The shot noise analysis is based on the relationship between frequency response to sinusoidal flickering light and noise characteristics during steady illumination (Dodge et al., 1968). This analysis suggests that the bumps (noise) which are superimposed on the generator potential are the building blocks of the potential. However, the shot noise model provides no information about spontaneous bumps. Therefore, it is desirable to verify this hypothesis by an approach which can relate the spontaneous bumps to light-induced bumps.

Yeandle and Spiegler (1973) reported recently that recordings from the *Limulus* ventral eye show bimodal distribution of bump sizes. Spontaneous bumps, on the average, were smaller than light-induced bumps. These observations suggest that spontaneous and light-induced bumps are generated by different mechanisms. Srebro and Behbehani (1972), on the other hand, studied the temperature dependence of the quantum bump frequency in the lateral eye of *Limulus* and came to the conclusion that spontaneous bumps result from thermal isomerization of visual pigment molecules. In their view, both spontaneous and light-induced bumps result from isomerization of visual pigment molecules.

In *Limulus* lateral eyes two different populations of spontaneous bumps, slow rising, small bumps and fast rising, large bumps, have been reported (Adolph, 1964; Borsellino and Fuortes, 1968). These two physiologically distinct populations render any analysis of the statistical relationship between spontaneous bumps and light-induced potentials extremely difficult. Thus, one of the objectives of the present experiments was to study the relationship between spontaneous and light-induced bumps as well as the relationship between the bumps and the generator potential in the fruitfly photoreceptors, which seem to have only one population of bumps.

If the principle of univariance holds, one would expect that the amplitude of bumps would not depend on wavelength and that the absorption spectrum of visual pigment (and hence the spectral sensitivity of the receptor potential) would coincide with the spectral variation in the efficiency of eliciting quantum bumps by incident photons. Adolph (1968) has measured the spectral sensitivity of quantum bump frequency in *Limulus* lateral eyes. The spectral sensitivity matched the Dartnall nomogram at wavelengths longer than 520 nm but deviated from the nomogram at shorter wavelengths. The degree of deviation increased with stimulus intensity. No satisfactory explanation was given for the deviation at shorter wavelengths. On the other hand, Spiegler's (1973) more recent measurements of the quantum bump frequency of *Limulus* ventral eyes at four different wavelengths showed that the relative spectral sensitivities at these points could be fitted by a Dartnall nomogram. The results did not differ significantly from Murray's (1966) absorption difference spectrum of *Limulus* photolabile pigment. Moreover, Spiegler found that the averaged bump shape and the height distribution of the quantum bumps

were roughly invariant at the four wavelengths investigated. Thus, Spiegler's results tended to support the idea of univariance while Adoph's did not. Therefore, our second objective was to investigate the relationship between spectral variation in efficiency of quantum bump production and spectral sensitivity of the generator potential. The following assumptions were examined: (*a*) Each effectively absorbed photon, regardless of its wavelength, produces bumps of the same mean size as spontaneous bumps; (*b*) Spectral dependence of the probability that an incident photon generates a bump corresponds to the spectral sensitivity of the receptor potential.

METHODS

White-eyed mutants (*w* or *bw;st*) of *Drosophila melanogaster* were used throughout these experiments to prevent the eye color pigments from interfering with spectral sensitivity measurements. The insects were mounted with the ventral side facing up. The ventral part of the head was sliced off with a vibrating razor blade to expose a horizontal section of the eye, the plane of section being roughly parallel to the long axes of the retinula cells. To prevent dessication, the sliced eye was submerged in saline (saline used by Ephrussi and Beadle [1936] buffered at pH 7.5) while the abdomen and thorax of the animal were kept free of saline by means of a wax barrier (Fig. 1). In this manner, respiration and circulation could be maintained with ease for 3–4 h. The light stimulus and the recording electrode were introduced perpendicular to the plane of the slice. The monochromatic light stimulus originated from a Bausch and Lomb High Intensity Monochromator (Bausch & Lomb Inc., Rochester, N. Y.) and had a half peak bandwidth of 8 nm. The investigations were carried out in the spectral range 400–600 nm. The ultraviolet light intensity was not high enough to extend the experiments into that region. The glass capillary microelectrodes were filled with 2 M KCl and had resistances of approximately 150 MΩ. The stimulus

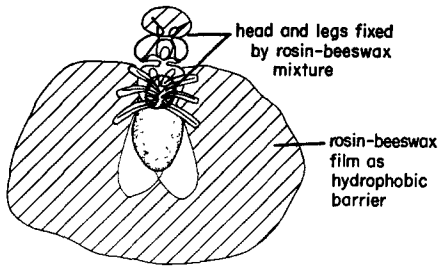

FIGURE 1. Preparation of the specimen. A hydrophobic rosin-beeswax mixture was used to mount the fly on a glass cover slip. The head and wings were fixed to the cover slip so that the ventral side was up, and legs were immobilized by a drop of the mixture. A film of the hydrophobic mixture was then applied around the abdomen and thorax. To expose the receptor cell layer for penetration with microelectrodes, the ventral part of the eyes was sliced off by a vibrating razor blade (driven by a loudspeaker of frequency ≃500 Hz). The sliced head was immediately submerged in saline to prevent dessication. Because of the hydrophobic film, the thorax and abdomen were kept free from the saline and respiration was maintained.

intensity was controlled by a pair of neutral density wedges. The intensity of the unattenuated, monochromatic stimulus light was measured at each wavelength using a Gamma Scientific spectroradiometer (Gamma Scientific, Inc., San Diego, Calif.). The transmission characteristics of the neutral density wedges were calibrated on a Shimadzu model MPR-50L spectrophotometer (Shimadzu Seisakusho Ltd., Kyoto, Japan) at each of the wavelengths used in this work. These calibrations allowed us to calculate the amount of attenuation due to the neutral density wedges at any given wedge settings. The attenuated stimulus intensities were also checked with the spectroradiometer at several wedge settings for each wavelength. For the experiments illustrated in Fig. 4 and Table I, the 10-ms, 500-nm stimulus flashes cast 10^{10} to 10^{11} photons/cm^2·s on the preparation. An ordinary dissecting lamp was used in preparing the animal for recording. Once an active unit was penetrated, dark adapting the preparation for 10–15 min was sufficient to allow one to begin recording bumps. Penetration of photoreceptors was facilitated either by using an electromagnetic jolter (Tomita et al., 1967) or by turning the negative capacitance control of the preamplifier to induce brief electronic oscillations (Baylor et al., 1971).

The signals picked up by the electrodes were displayed on an oscilloscope and recorded on a Brush pen recorder (Gould Inc., Cleveland, Ohio) and also on magnetic tape for subsequent playback. The data shown in Figs. 2, 3, 5, 6, 7, and 9 were obtained from pen recorder tracings. The Brush pen recorder has a high frequency cutoff of about 100 Hz. In the above recordings, however, a low pass filter having a high frequency cutoff of 40 Hz was used to reduce 60-cycle and Johnson noises. When needed, a PDP 12 Digital Computer (Digital Equipment Corp., Maynard, Mass.) was used for signal averaging. Because of the high resistance electrodes required for the penetration of small cells, the noise level of recordings was relatively high, and stable recordings were difficult to obtain. Only a small fraction (< 10%) of the penetrated cells yielded stable enough recordings for a long enough period (0.5–1.0 h) to allow the type of analysis reported here. Results were discarded if the resting membrane potential drifted by more than 2 mV in any of the experiments.

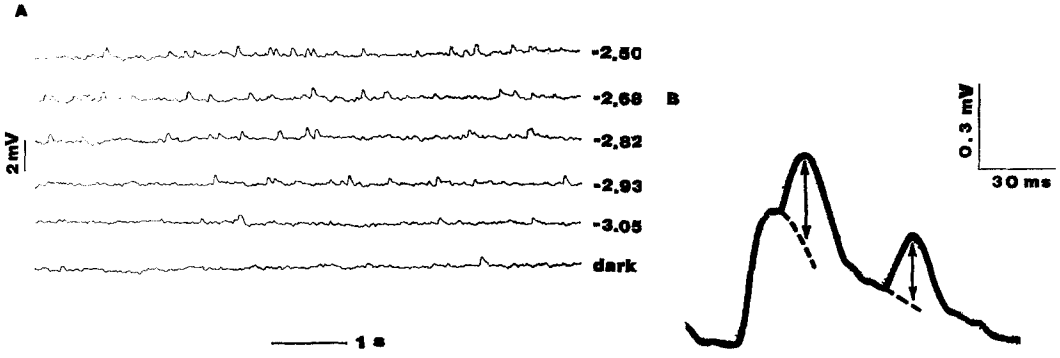

FIGURE 2. (A) Intracellularly recorded bumps in photoreceptors of *Drosophila melanogaster* under conditions of increasing light stimulus. Numbers indicate the relative intensity of the stimulus in log scale (450 nm). (B) A recording showing bump superposition. The exponential decay of the bumps was extrapolated and the amplitudes (arrows) of the superimposing bumps were measured from the extrapolated base lines. The record was taken from a pen recorder tracing.

The amplitudes of bumps decreased continuously into the noise level. Therefore, voltage fluctuations were accepted as bumps only if their duration exceeded 30 ms and if their amplitude exceeded about twice that of the noise level. Since bumps displayed a characteristic waveform, lasting for 30 ms or more, and noise consisted mainly of 60 cycles, differentiating the bumps from noise was not as formidable as it might have been. In the case of superposed bumps, the exponential decay of the first bump was extrapolated, and the amplitude of the second bump was measured from the extrapolated base line, as illustrated in Fig. 2 B (see, for example, Katz, 1966).

The spectral sensitivity of the receptor potential was obtained from intracellular recordings on three cells and electroretinogram (ERG) recordings on six flies (criterion response = 1.0 mV). The spectral sensitivities obtained by these two recording techniques were similar, and the data were combined.

RESULTS AND DISCUSSION

Spontaneous and Light-Induced Bumps of Drosophila Photoreceptors

Spontaneous discrete bumps of 0.2–1.0-mV amplitude could be recorded intracellularly from a *Drosophila* retinula cell, if the preparation had been dark adapted for at least 10–15 min (Fig. 2 A). As in the case of other preparations (Fuortes and Yeandle, 1964; Scholes, 1965), the spontaneous bumps of *Drosophila* retinula cells appeared to occur randomly, since the intervals between successive bumps could be approximated by an exponential distribution (Fig. 3). In response to dim light, light-induced bumps began to contribute, and consequently the frequency of bumps increased (Fig. 2 A, B).

The effects of summing bumps induced by successive dim stimulus flashes are illustrated in Fig. 4 A and B. These figures show computer-averaged responses of two different photoreceptor cells to dim stimulus flashes of 10-ms

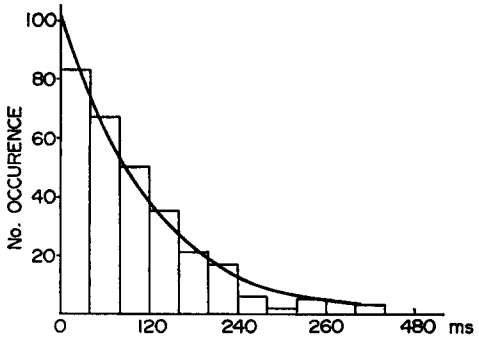

FIGURE 3. Distribution of the interval between successive spontaneous bumps. An exponential curve was fitted to the histogram. χ^2 test of goodness of fit was carried out. The degree of freedom (df) was determined by the number of tested classes minus 2, because the total number (289) and the mean (120 ms) of the histogram were used to construct the exponential distribution. The χ^2 value is 13.07 with df = 8, giving a significance level between 0.10 and 0.20. (From the 10th class on, all residual classes were combined.)

duration. Stimulus flashes of 475-, 500-, and 575-nm wavelengths were used for the cell shown in Fig. 4 A, and 500- and 550-nm wavelengths were used for the cell shown in Fig. 4 B. In each case, the averaged responses to stimuli of different wavelengths were normalized and superposed on each other for comparison. It may be seen that the waveform of the averaged responses varied from cell to cell but appeared to be largely independent of stimulus wavelength in a given cell. Note also that the averaged responses returned to the base line in about 100 ms.

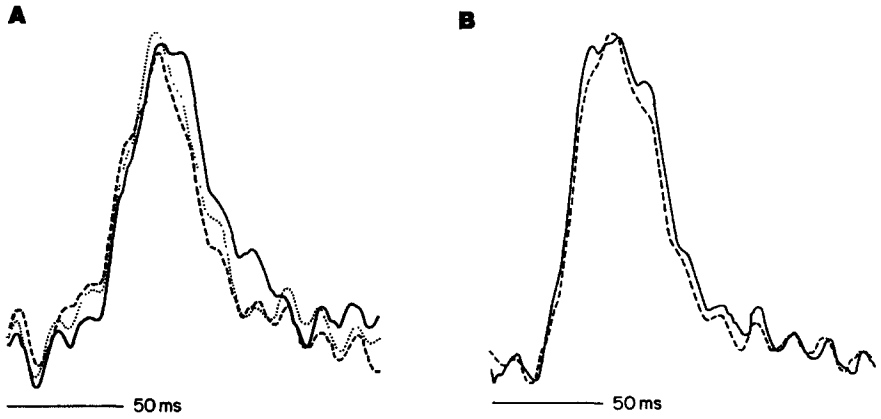

FIGURE 4. Computer-averaged responses to 10-ms, low intensity flashes at various wavelengths. Flash frequency = 0.66/s. Traces begin at the onset of stimulation. Averaged signals from the same cell were normalized with respect to peak-to-peak amplitude and superposed to facilitate comparison. Small ripples on the traces are the remaining 60-cycle noise. (A) Averaged responses to stimuli of 475 nm (continuous line), 500 nm (dashed line), and 575 nm (dotted line) from the same cell. Number of responses averaged: 74, 75, and 90 for 475, 500, and 575 nm, respectively. (B) Averaged responses from another cell. Continuous line: 500 nm; dashed line: 550 nm. Number of responses averaged: 65 for 500 nm and 89 for 550 nm.

Using our selection criteria for bumps, we found no evidence for bimodal distribution of spontaneous bumps in *Drosophila*. There were no large bumps corresponding to the regenerative, fast-rising bumps reported in *Limulus* (Adolph, 1964; Dowling, 1968). Moreover, to a first approximation at least, the amplitude histogram of *Drosophila* spontaneous bumps fitted a Gaussian (Fig. 5, insets). Because of these properties, *Drosophila* bumps appeared to be well suited for the analysis of the relationship between the spontaneous bumps and the light-induced potential. In particular, the hypothesis that spontaneous bumps are the quantal units of the receptor potential could be tested using an approach similar to that applied to the miniature end-plate potential of the neuromuscular junction (del Castillo and Katz, 1954; Boyd and Martin, 1956).

Spontaneous Bumps as Quantal Units of Light-Induced Potentials

The purpose of these experiments was to test the hypothesis that each response to a stimulus flash consists of an integral number of units which are statistically indistinguishable from spontaneous bumps. If the stimulus intensity is sufficiently low, the individual bumps contained in a response can be distinguished, and the number of these bumps is expected to vary according to the Poisson statistics. Therefore, the idea was to construct the amplitude distribution of the response using Poisson statistics under the assumption that the quantal units of response have the same mean size and variance as the spontaneous bumps and then see how this distribution compares with the experimentally determined amplitude distribution.

Stimuli in these experiments consisted of trains of low intensity monochromatic flashes. Each train contained 61–147 flashes of 10-ms duration presented about 1.5 s apart. For each cell studied, stimuli of two different wavelengths were applied.

The number of photons contained in each dim flash impinging upon a cell fluctuates randomly about a mean value determined by the output of the light source and the attenuation of the stimuli. The probability distribution of the number of photons in each flash is described by the Poisson distribution:

$$P_k = \frac{(\lambda t)^k}{k!} \exp(-\lambda t);\ k = 0, 1, 2, \cdots, \qquad (1)$$

where P_k is the probability that exactly k photons are contained in a flash, λ is the mean number of quanta delivered by the stimulus flash per unit time, t is the duration of flash, and therefore λt is the mean number of quanta in each flash. If the probability that an incident photon of a given wavelength is effective in generating a light-induced bump is denoted by δ, then the probability distribution for the number of effective quanta will still be a Poisson distribution with $\delta\lambda t$ replacing λt in Eq. 1. However, spontaneous bumps also contribute to the total number of bumps in a response. If the rate of spontaneous bump generation is λ' (average number per unit time), then the probability distribution of the number of spontaneous bumps generated in the period t' (100-ms period after the onset of the flash) is also a Poisson distribution with parameter $\lambda' t'$, since the time of occurrence of a spontaneous bump is random. (A 100-ms period was chosen for t', because, as we have seen previously, with dim stimuli of 10-ms duration, most of the light-induced responses occurred within 100 ms (Fig. 4 A and B)). One of the features of the Poisson process is that a combination of two independent Poisson processes is another Poisson process with the sum of the two parameters as the new parameter (Feller, 1968). Consequently, the probability

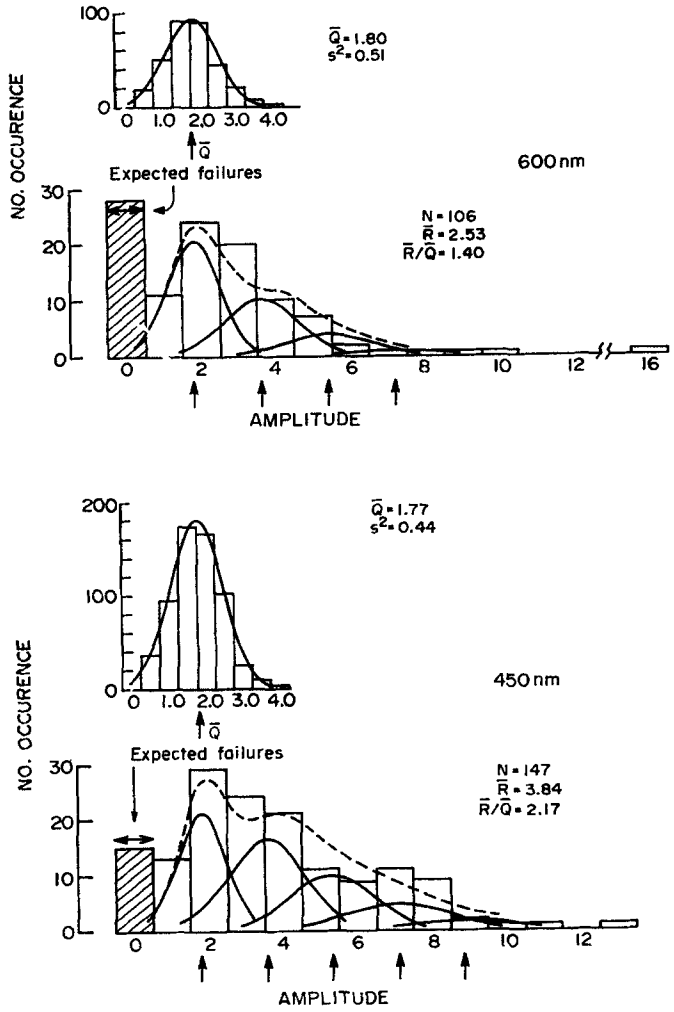

FIGURE 5. Amplitude histograms of spontaneous bumps and responses to 10-ms low intensity flashes. All data are from the same cell (C5). Stimulus wavelengths: 450 and 600 nm. Spontaneous bumps were recorded during last 600-ms periods of the 1.5-s intervals between flashes. Normal curves, whose areas correspond to the calculated number of events in each Poisson class, are centered at integral multiples of the mean amplitude of the spontaneous bumps (see text). The sum of these normal curves (dashed curves) indicates the expected distribution of response amplitude. The expected number of failures is indicated. The observed number of failures is expressed as the height of the hatched rectangle. Distributions of spontaneous bumps are shown in the insets. Normal curves with the indicated means ($\bar{Q}$) and variances (s^2) are fitted to the histograms. For the upper histogram (600-nm case) 329 spontaneous bumps were used, and for the lower histogram (450-nm case) 613 spontaneous bumps were used. Estimated spontaneous bump content ($\lambda' t'$, see text) in the response to 450- and 600-nm stimuli were 0.70 and 0.52, respectively. Amplitude axes of all histograms are in the same scale. One amplitude unit = 0.08 mV. N = number of trials or number of flashes applied. $\bar{R}$ = mean ampli-

distribution of the number of bumps, both light induced and spontaneous, occurring in the period t' is a Poisson distribution having a mean of $\delta\lambda t + \lambda' t'$. The quantity $\delta\lambda t + \lambda' t'$ represents the average number of bumps produced in interval t', both spontaneously and induced by light stimulus of duration t (where $t < t'$).

We now define the amplitude of a response (denoted by R) as the sum of the amplitudes of indivudual bumps, both spontaneous and light induced, occurring in t', the 100-ms period after the onset of each flash. In this definition of R, the amplitude of each bump is measured separately, using the procedure outlined in Methods, and summed together. The response amplitude, so defined, is not to be confused with the computer-summed amplitudes shown in Fig. 4 A and B. In the latter case, a large number of responses were summed together without correcting for latency dispersion of individual bumps and, hence, without having to identify individual bumps in a response.

The stimulus intensity was kept low so that, on the average, no more than about two light-induced bumps were produced by any given stimulus flash. At these low levels of illumination, the bumps are expected to sum linearly. The histograms in Fig. 5 illustrate the distribution of the response amplitudes, R, obtained from the same cell in response to 450- and 600-nm flashes. $\bar{R}$'s are the mean values of the histograms, or the mean response amplitudes, obtained in 106 and 147 trials at 600 and 450 nm, respectively. ($\bar{R}$ = 3.84 arbitrary units or 0.31 mV at 450 nm, and 2.53 U or 0.20 mV at 600 nm).

The amplitude distribution of spontaneous bumps occurring in the dark (last 600-ms periods of the 1.5-s intervals between flashes) is displayed in the histograms shown in the insets of Figs. 5 A and B. The mean amplitude of the spontaneous bumps, $\bar{Q}$, and their variance, s^2, were calculated from the histogram ($\bar{Q}$ = 1.80 arbitrary units at 600 nm, and 1.77 at 450 nm; s^2 = 0.51 at 600 nm, and 0.44 at 450 nm).

Since the number of bumps in a response is expected to obey the Poisson statistics (Eq. 1), the expected frequency of occurrence of a response containing exactly k bumps in a total of N responses to N flashes is given by

$$NP_k = N \cdot \frac{(\delta\lambda t + \lambda' t')^k}{k!} \exp\{-(\delta\lambda t + \lambda' t')\}, \qquad (2)$$

---

tude of responses to the dim flash. χ^2 tests of goodness of fit for the response amplitude distributions were performed. Classes in the tail end of the histogram were combined. The degrees of freedom (df) were determined by number of tested classes minus 3, because, in addition to total number of trials, the mean and variance of spontaneous bumps were used to construct the expected distribution. For the 600-nm data, χ^2 = 4.42 with df = 5 giving a significance level (α) between 0.40 and 0.50. (From the eighth class on, all residual classes were combined.) For 450-nm data, χ^2 = 8.79 with df = 7 and $0.20 < \alpha < 0.30$. (From the 10th class on, residual classes were combined).

where all quantities have been defined previously. If, indeed, the quantal units of a response are indistinguishable from the spontaneous bumps, the parameter $\delta\lambda t + \lambda' t'$ may be replaced by the ratio $\bar{R}/\bar{Q}$, and we have

$$NP_k = N \cdot \frac{(\bar{R}/\bar{Q})^k}{k!} \cdot \exp(-\bar{R}/\bar{Q}), \tag{3}$$

where $\bar{R}$ is the mean response amplitude and $\bar{Q}$ is the mean amplitude of spontaneous bumps. Moreover, since the spontaneous bumps appear to be normally distributed with the mean and variance given by $\bar{Q}$ and s^2, respectively (insets, Figs. 5, 6, and 7), the amplitude distribution of responses which contain exactly k bumps should center normally about the mean $k\bar{Q}$ with the variance ks^2. The sum (dashed curves in Fig. 5) of these individual distributions (solid curves in Fig. 5) gives the expected amplitude distribution of the N responses which may contain 1, 2, . . . bumps (for detail see del Castillo and Katz, 1954).

Figs. 6 and 7 show similar treatments of the responses of other cells to flashes of other wavelengths. Note that $\bar{Q}$ and s^2 remained roughly constant for each cell when two different wavelengths were applied. In all experiments analyzed, the theoretical curves fitted the experimental histograms reasonably well (Figs. 5, 6, and 7). Moreover, the expected number of failures, i.e. the probability that no bump is contained in a response, also fitted the experimental histograms (Figs. 5, 6, and 7).

These results suggest that both the spontaneous and light-induced bumps are produced by the same mechanism and that the spontaneous bumps are the quantal units of the light-induced receptor potential.[1] In addition, the data are consistent with the notion that photons of different wavelengths produce the same effect when effectively absorbed, since for each cell essentially the same quantal unit (no significant difference in $\bar{Q}$ and s^2) could be used to construct the theoretical curves at the two wavelengths (Figs. 5, 6, and 7).

Variation in Probability of Light-Induced Bump Production at Different Wavelengths

Three different approaches were used to test if the effectiveness of eliciting bumps by light of different wavelengths varied according to the spectral sensitivity of the receptor potential. In the first approach, the relative efficiency of quantum bump production at various wavelengths was evaluated by the signal-averaging technique.

Experiments consisted of summing the responses to the repeated 10-ms

[1] This is not intended to imply necessarily that isomerization of visual pigment molecules is involved in the generation of both types of bumps as suggested by Srebro and Behbehani (1972).

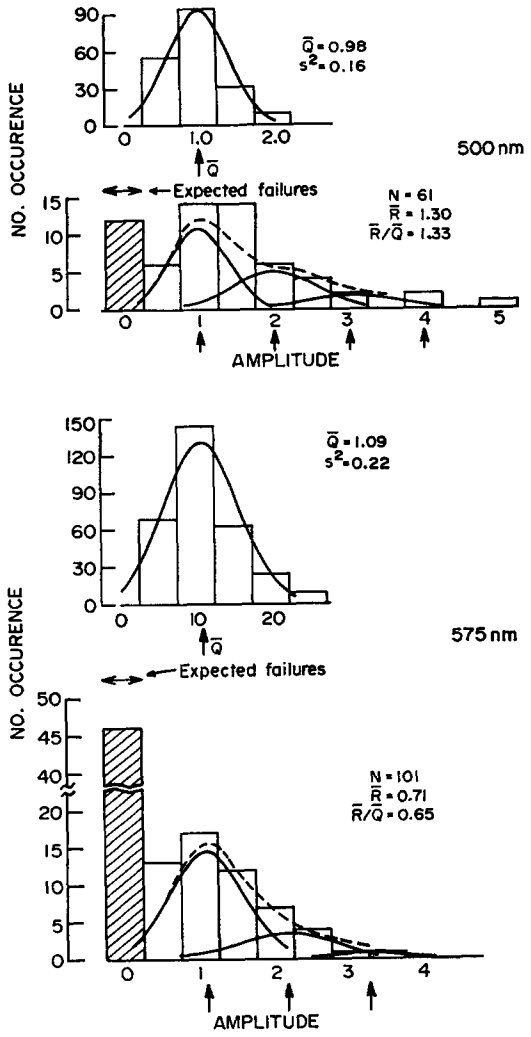

FIGURE 6. Amplitude histograms and expected distributions for another cell. Stimulus wavelengths: 500 and 575 nm. $\lambda' t'$ = 0.30 and 0.38 for 500- and 575-nm histograms, respectively. One amplitude unit = 0.43 mV. For 500-nm data χ^2 = 5.21 with df = 4 and $0.20 < \alpha < 0.30$. (From seventh class on all residual classes were combined.) For 575-nm data χ^2 = 3.76 with df = 3 and $0.20 < \alpha < 0.30$. (From the sixth class on, the residual classes were combined.)

stimuli (presented about 1.5 s apart) over a large number of trials (stimuli). The number of trials over which the averaging was carried out varied from 65 to 185. In each experiment, the intensity of the stimulus flashes was so adjusted that no bumps were produced in more than about 15% of trials. In this way the stimulus intensity was held to an approximate "constant response"

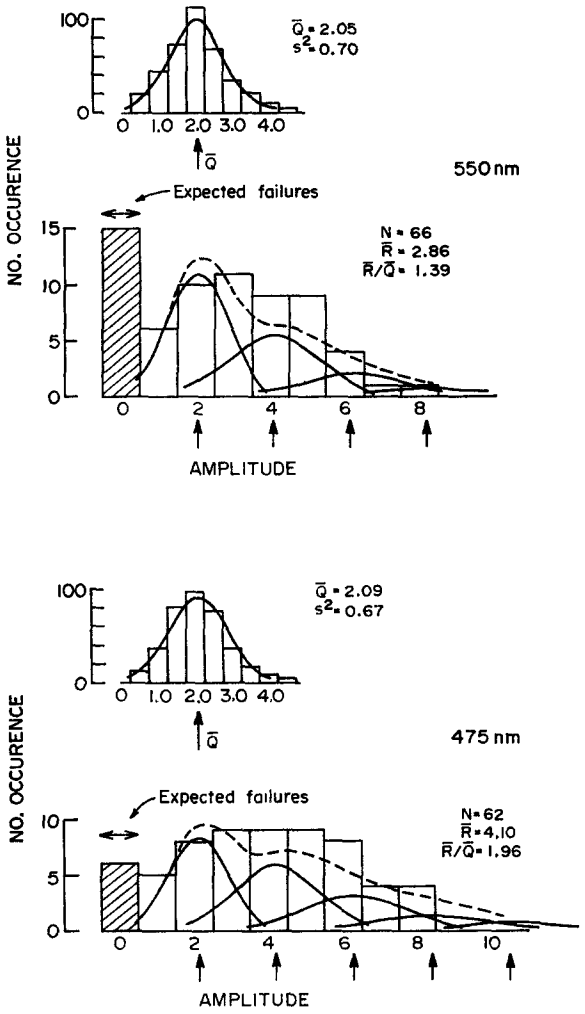

FIGURE 7. Amplitude histograms and expected distributions for still another cell. Stimulus wavelengths: 475 and 550 nm. $\lambda' t'$ was 0.99 in both cases. For 475-nm data $\chi^2 = 5.16$ with df = 5 and $0.40 < \alpha < 0.50$. (From the eighth class on, the residual classes were combined.) For 550-nm data $\chi^2 = 3.88$ with df = 4 and $0.40 < \alpha < 0.50$. (From seventh class on all residual classes were combined.)

level. In this intensity range, a large quantal fluctuation was prominent in the response, and according to the Poisson law, the chance of having more than three bumps in a given trial was relatively small. Therefore, it was reasonable to expect the responses to remain in the linear range. (Note that quantum bumps are less than 1 mV in amplitude, while the saturated amplitude of the receptor potential exceeds 30 mV.) Over a large number of trials, spontaneous

bumps, which are random and independent in occurrence, sum up to a constant dark level. The area above the dark level, therefore, is proportional to the total number of light-induced bumps elicited in all trials. The area so obtained was then divided by the number of trials to yield an "averaged response." Fig. 4 shows the typical averaged responses to stimuli of several different wavelengths. In order to compare the relative efficiency of bump production at different wavelengths, the area of the averaged response (A_i) obtained from a given cell at each wavelength (ϕ_i) was divided by the number of photons (m_i) impinging on the preparation per unit time per unit area at that wavelength. The areas of the averaged responses adjusted in this way, i.e. A_i/m_i, served as indicators of the effectiveness of photons in producing light-induced bumps at any given wavelength ϕ_i. Thus to obtain the ratio of efficiency in light-induced bump production at any two wavelengths, one had only to take the ratio of the adjusted areas of the averaged responses obtained from the same cell at those two wavelengths (e.g. $(A_1/m_1)/(A_2/m_2)$ at ϕ_1 and ϕ_2).

Table I shows the results of the above analysis on the relative efficiency of quantum bump production at six pairs of wavelengths. For each pair of wavelengths, data from three or more cells have been collected, expressed in log units, and listed in the table as group X_2. Groups X_1 are the differences in the spectral sensitivity of the receptor potential at the specified pairs of wavelengths also expressed in logarithmic units. The following statistical treatment was used to test for any significant difference in the means of these two populations. If we assume that the two populations being tested are normally distributed with similar variances,[2] then the difference between the means $(\overline{X}_1 - \overline{X}_2)$ of the two samples, each taken from one of the two populations, is also normally distributed, and the ratio of the difference between the sample means over the standard error of the difference between the means, $(\overline{X}_1 - \overline{X}_2)/(s_{\bar{x}_1 - \bar{x}_2})$, is distributed as Student's t with $n_1 + n_2 - 2$ degrees of freedom, where n_1 and n_2 are the sample sizes. The quantity $s_{\bar{x}_1 - \bar{x}_2}$ is calculated from the equation

$$s^2_{\bar{x}_1 - \bar{x}_2} = \frac{(n_1 - 1)s_{x_1}^2 + (n_2 - 1)s_{x_2}^2}{n_1 + n_2 - 2}(1/n_1 + 1/n_2),$$

where $s_{x_1}^2$ and $s_{x_2}^2$ are the sample variances.

The last two columns in Table I list the t values, $(\overline{X}_1 - \overline{X}_2)/(s_{\bar{x}_1 - \bar{x}_2})$, and the 95% critical values ($t_{0.975}$) for t distribution with $n_1 + n_2 - 2$ degrees of

[2] Based on the sample variances of the data in Table I, $s^2_{\bar{x}_1}$ and $s^2_{\bar{x}_2}$, the F tests for the significant difference in the population variances were carried out. The data for the 500–500-nm pair of wavelengths exhibited no significant difference in variance at the 1% level. The differences in variances for other pairs of data were not significant at the 5% level.

TABLE I

COMPARISON BETWEEN SPECTRAL SENSITIVITY OF RECEPTOR POTENTIAL AND SPECTRAL VARIATIONS IN EFFICIENCY OF QUANTUM BUMP PRODUCTION

Wavelength	Cell or fly no.	Log difference (X)*	Mean ($\bar{X}$)	Standard deviation (s_X)	$\lvert \bar{X}_1‡ - \bar{X}_2§ \rvert$	$s_{\bar{X}_1-\bar{X}_2}$‖	t Value¶	$t_{0.975}$**
nm								
450	C2	2.13						
600	C4	2.37						
	F1	1.87						
X_1	F2	1.96	2.09	0.15				
	F3	2.04						
	F4	2.12						
	F5	2.17			0.07	0.099	0.71	2.23
	F6	2.05						
	C5	1.90						
X_2	C13	2.02	2.02	0.12				
	C14	2.14						
475	C2	0.75						
550	C4	0.88						
	C5	0.98						
	F1	0.86						
X_1	F2	0.53	0.81	0.13				
	F3	0.80						
	F4	0.80						
	F5	0.92			0.01	0.077	0.13	2.20
	F6	0.79						
	C8	0.72						
	C9	0.98						
X_2	C11	0.91	0.82	0.15				
	C18	0.68						

* Log difference in the spectral sensitivity of the receptor potential or in the efficiency of quantum bump production.

‡ Relative spectral sensitivity of the receptor potential obtained either intracellularly (C) or extracellularly (F).

§ Relative area of the averaged response (see text).

‖ Estimated standard deviation of the difference between the population mean values of samples X_1 and X_2, estimated by

$$s_{\bar{X}_1-\bar{X}_2} = \left[\frac{(n_1-1)s_{X_1}{}^2 + (n_2-1)s_{X_2}{}^2}{n_1+n_2-2}\left(\frac{1}{n_1}+\frac{1}{n_2}\right)\right]^{1/2},$$

where n_1, n_2, X_1, X_2, and $s_{\bar{X}_1}$, $s_{\bar{X}_2}$ are the sample sizes, means and standard deviations of groups X_1 and X_2, respectively.

¶ Obtained from $\lvert {}_1\bar{X} - \bar{X}_2 \rvert / s_{\bar{X}_1-\bar{X}_2}$.

** The critical t value such that $Pr\{\lvert t \rvert \geq t_{0.975}\} = 0.05$ in the t distribution with $n_1 + n_2 - 2$ df.

TABLE I—(*Continued*)

Wavelength	Cell or fly no.	Log difference (X)*	Mean ($\bar{X}$)	Standard deviation (s_X)	$\lvert \bar{X}_1 - \bar{X}_2 \rvert$	$s_{\bar{X}_1-\bar{X}_2}$	t Value¶	$t_{.975}$**
nm								
500	C2	0.29						
400	C4	0.17						
	F1	0.33						
	X_1 F2	0.25	0.36	0.17				
	F3	0.27						
	F4	0.41						
	F5	0.67						
	F6	0.55			0.16	0.083	1.92	2.16
	C3	0.58						
	C12	0.52						
	C14	0.71						
	X_2 C15	0.50	0.52	0.14				
	C16	0.37						
	C17	0.64						
	C18	0.33						
500	C2	0.66						
550	C4	0.72						
	C5	0.82						
	F1	0.84						
	X_1 F2	0.49	0.72	0.11				
	F3	0.70						
	F4	0.72						
	F5	0.84						
	F6	0.69			0.11	0.118	0.93	2.23
	C10	0.76						
	X_2 C11	1.17	0.83	0.31				
	C18	0.55						
500	C2	1.38						
575	C4	1.72						
	C5	1.46						
	F1	1.38						
	X_1 F2	1.20	1.44	0.15				
	F3	1.46						
	F4	1.44						
	F5	1.60						
	F6	1.35			0.08	0.098	0.82	2.18
	C6	1.36						
	C7	1.07						
	X_2 C10	1.75	1.36	0.25				
	C11	1.29						
	C18	1.32						
550	C2	1.00						
575	C4	0.64						
	C5	0.72						
	F1	0.54						
	X_1 F2	0.71	0.72	0.13				
	F3	0.77						
	F4	0.72						
	F5	0.76						
	F6	0.65			0.04	0.121	0.33	2.23
	C10	0.98						
	X_2 C11	0.54	0.76	0.22				
	C18	0.75						

freedom. It is clear from Table I that none of the differences between the pairs of means under test is significant at the 5% level.

Fig. 8 summarizes the results presented in Table I. Open circles represent the relative spectral sensitivity of the receptor potential (obtained from the same data from which groups X_1 in Table I were derived). A Dartnall nomogram peaking at 485 nm was plotted against the data points for comparison. Since we were able to obtain averaged responses at only two wavelengths from most of the cells, the data shown in Table I were plotted in Fig. 8 pair by pair, to be described below. For each set of data in Table I, the probability of quantum bump production was arbitrarily set equal to the sensitivity of the receptor potential at one of the wavelengths. Thus, the difference in the means of these two quantities and the standard error of the difference between the two means ($s_{\bar{X}_1-\bar{X}_2}$) were made to appear at the other wavelength, the latter quantity appearing as error bars. For example, open triangles in Fig. 8 repre-

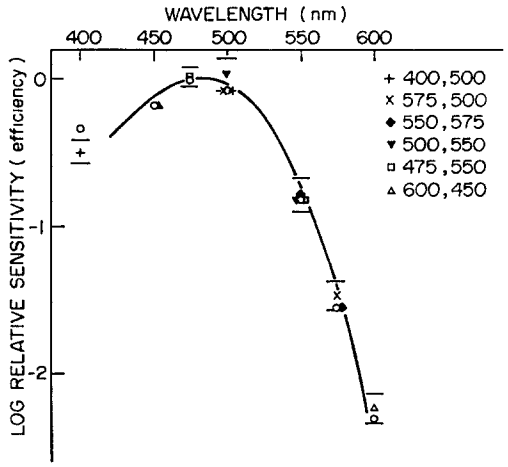

FIGURE 8. Summary plot of the data in Table I. Open circles correspond to the log relative sensitivity of the receptor potential. The same data from which groups X_1 in Table I were derived, were used to obtain these data points. The continuous curve is a Dartnall nomogram peaking at 485 nm. The measured spectral sensitivity of 400 nm substantially deviates from the nomogram, because of the large UV peak present in dipteran, but not in vertebrate, spectral sensitivity curves. As shown in the legend, symbols other than circles were used to plot the relative efficiency in quantum bump production at each pair of wavelengths (mean values of groups X_2 in Table I). The relative sensitivity at the second wavelength of each pair shown in the legend (e.g. 450 nm for the last pair denoted by open triangles) was set equal to the relative sensitivity of the receptor potential at the same wavelength (open circle). The difference in the mean values ($\bar{X}_1 - \bar{X}_2$) of the two quantities, thus, appeared at the other wavelength (600 nm in this case). The error bars, representing the standard error of the difference between means ($s_{\bar{X}_1-\bar{X}_2}$), were also placed at the first wavelength of each pair. Note that, except for the last pair (450 and 600 nm), all pairs of wavelengths under test are interconnected with each other.

sent the relative efficiency of quantum bump production at 450 and 600 nm plotted from the group X_2 of the first set of data in Table I. The efficiency of quantum bump production was set equal to the sensitivity of the receptor potential at 450 nm. The deviation between the means of the two quantities $(\overline{X}_1 - \overline{X}_2)$ is shown at 600 nm. The deviation (0.07 log units) is smaller than 1 SE of the difference between the two means.

In a few cases (C11, C18, etc. in Table I), it was possible to measure the averaged responses to more than three wavelengths from single cells. In these cases, the relative efficiency of bump production could be compared to the spectral sensitivity directly without resorting to the above strategy. Although, as one might expect, individual data points showed greater scatter than those shown in Fig. 8, they, nevertheless, closely followed the spectral sensitivity curve (not shown).

The second approach to evaluate the probability of light-induced bump production was to analyze the bump amplitude histograms shown in Figs. 5, 6, and 7. The analysis was carried out in four cells, each at a different pair of wavelengths (Table II, third column). At each wavelength, the number of light-induced bumps was determined by subtracting the average number of spontaneous bumps generated during t' (100 ms) from the mean number of bumps contained in a response $\overline{R}/\overline{Q}$, i.e. $\delta\lambda t = \overline{R}/\overline{Q} - \lambda' t'$. The above results were subjected to the same corrections as in the first approach to enable comparison of the relative efficiency in generating bumps at the two wavelengths.

TABLE II

COMPARISON OF SPECTRAL VARIATIONS IN THE EFFICIENCY OF QUANTUM BUMP PRODUCTION OBTAINED BY THREE DIFFERENT METHODS

		Log (δ_1/δ_2)		
Wavelength	Cell no.	Amplitude histograms*	($f - \lambda'$) vs. λ‡	Signal averaging (mean ± SD)§
nm				
500 575	C1	1.10	—	1.36±0.25
500 400	C3	0.67	—	0.52±0.14
475 550	C4	0.60	0.66	0.82±0.15
450 600	C5	1.90	2.00	2.02±0.12

* $\delta\lambda t = \overline{R}/\overline{Q} - \lambda' t'$ (see Figs. 5, 6, and 7).

‡ Data shown in Fig. 9.

§ Data processed as shown in Table I.

Table II, third column, shows the relative probability of light-induced bump production at four pairs of wavelengths obtained by this method and expressed in log units.

In the third approach, the wavelength dependence of the probability of light-induced bump production was evaluated by measuring the rate of bump production under steady illumination as a function of stimulus intensity at two pairs of wavelengths (Fig. 9). The rate of bump generation is the sum of the rates of spontaneous and light-induced bumps. Since the rate of light-induced bumps is proportional to light intensity, we can relate the frequency of bump generation, f, to intensity, λ, by the equation $f = \delta\lambda + \lambda'$, where λ' is the rate of spontaneous bump production in the dark and δ is the proportionality constant at the wavelength of incident quanta. Note that λ is expressed in number of photons per unit time. It follows that $\log (f - \lambda') = \log \lambda + \log \delta$. The function $f - \lambda'$, or the rate of light-induced bumps, will appear as a straight line with slope 1 when plotted against λ in a double log plot. The constant term $\log \delta$ will be the intercept of the curve with the λ axis. If light stimuli of two different wavelengths are applied in separate experiments, the plots become two parallel lines, and the difference in their intercepts, $\log \delta_1 - \log \delta_2 = \log \delta_1/\delta_2$, would indicate the relative effectiveness of bump production at those two wavelengths. Fig. 9 shows two pairs of $\log (f - \lambda')$ vs. $\log \lambda$ lines observed in two different cells. The straight lines of slope 1 were fitted to the experimental data by eye and the separation between each pair of lines, $\log \delta_1/\delta_2$, was evaluated. The results were entered in the fourth column of Table II.

Since recording the bumps in this preparation is technically difficult and

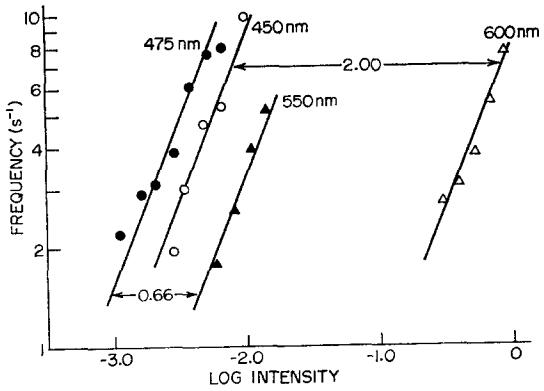

FIGURE 9. Rate of light-induced bumps ($f - \lambda'$) vs. light intensity (λ) at two pairs of wavelengths. The 475- and 550-nm data were obtained from the same cell, and 450- and 600-nm data from another cell. Lines of slope 1 are fitted to data points by eye. The horizontal separation between two lines, indicated by the arrows correspond to the relative efficiency of bump production, $\log (\delta_1/\delta_2)$ (see text).

time consuming, we decided to collect sufficient data for a reasonably rigorous statistical treatment only in the case of the first approach. The data obtained by this method (Table I) showed that the differences between the efficiency of quantum bump production and the spectral sensitivity of the receptor potential are not significant at the 5% level. Moreover, the values derived from all three methods were in reasonable agreement with each other. These data, taken together, support the hypothesis that the spectral sensitivity of the receptor potential has its origin in the relative efficiency or probability of bump production at different wavelengths. Thus, in the spectral range investigated (400–600 nm), photons of various wavelengths appear to be equivalent in eliciting quantum bumps as long as they are effectively absorbed by the visual pigment. The last statement is supported by our previous observation that the mean amplitude and variance of the quantal units of the receptor potential, i.e., spontaneous bumps, show little dependence on stimulus wavelength for any given cell studied (Figs. 5, 6, and 7). The same conclusion is also supported by the observation that the waveform of the computer-summed responses to dim flashes appear to be largely independent of stimulus wavelength (Fig. 4).

It should be noted that the second and third approaches involved identification of individual bumps, whereas in the first method, identification of individual bumps was not needed. The fact that the data derived from all three methods agree with each other (Table II) strengthens the validity of the criteria used for the identification of individual bumps (see Methods).

We thank Dr. J. T. Yates for the use of the computer and Drs. M. C. Deland, B. W. Knight, and L. H. Pinto for their criticism of the manuscript.
This work was supported by grants from NSF (GB-35316) and NIH (EY-00033).

Received for publication 24 October 1973.

REFERENCES

ADOLPH, A. R. 1964. Spontaneous slow potential fluctuations in the *Limulus* photoreceptor. *J. Gen. Physiol.* **48**:297.

ADOLPH, A. R. 1968. Thermal and spectral sensitivities of discrete slow potentials in *Limulus* eye. *J. Gen. Physiol.* **52**:584.

BAYLOR, D. A., M. G. F. FUORTES, and P. M. O'BRYAN. 1971. Receptive fields of cones in the retina of the turtle. *J. Physiol.* (*Lond.*). **214**:265.

BORSELLINO, A., and M. G. F. FUORTES. 1968. Responses to single photons in visual cells of *Limulus*. *J. Physiol.* (*Lond.*). **196**:507.

BOYD, I. A., and A. R. MARTIN. 1956. The endplate potential in mammalian muscle. *J. Physiol.* (*Lond.*). **132**:74.

DEL CASTILLO, J., and B. KATZ. 1954. Quantal components of the endplate potential. *J. Physiol.* (*Lond.*). **124**:560.

DODGE, F. A., B. W. KNIGHT, and J. TOYODA. 1968. Voltage noise in *Limulus* visual cells. *Science* (*Wash. D.C.*). **160**:88.

DOWLING, J. E. 1968. Discrete potentials in the dark-adapted eye of the crab *Limulus*. *Nature* (*Lond.*). **217**:28.

EPHRUSSI, B., and G. W. BEADLE. 1936. A technique of transplantation for *Drosophila*. *Am. Nat.* **70**:218.

FELLER, W. 1968. An Introduction to Probability Theory and Its Applications. Wiley & Sons, Inc. New York. **1**:170.

FUORTES, M. G. F., and S. YEANDLE. 1964. Probability of occurrence of discrete potential waves in the eye of *Limulus*. *J. Gen. Physiol.* **47**:443.

KATZ, B. 1966. Nerve, Muscle, and Synapse. McGraw-Hill Book Company, New York. 140.

KIRSCHFELD, K. 1966. Discrete and graded receptor potentials in the compound eye of the fly (*Musca*). *In* The Functional Organization of the Compound Eye. C. G. Bernhard, editor. Pergamon Press, Oxford.

MILLECCHIA, R., and A. MAURO. 1969. The ventral photoreceptor cells of *Limulus*. II. The basic photoresponse. *J. Gen. Physiol.* **54**:310.

MURRAY, G. C. 1966. Intracellular absorption difference spectrum of *Limulus* extra-ocular photolabile pigment. *Science* (*Wash. D.C.*). **154**:1182.

RUSHTON, W. A. H. 1972. Visual pigments in man. *In* Handbook of Sensory Physiology Vol. VII/1. H. J. A. Dartnall, editor. Springer-Verlag, Berlin.

SCHOLES, J. 1965. Discontinuity of the excitation process in locust visual cells. *Cold Spring Harbor Symp. Quant. Biol.* **30**:517.

SPIEGLER, J. B. 1973. Photoreceptor spatial properties. Ph.D. Thesis. Indiana University, Bloomington, Ind.

SREBRO, R., and M. BEHBEHANI. 1972. The thermal origin of spontaneous activity in the *Limulus* photoreceptor. *J. Physiol.* (*Lond.*). **224**:349.

TOMITA, T., A. KANEKO, M. MURAKAMI, and E. L. PAUTLER. 1967. Spectral response curves of single cones in the carp. *Vision Res.* **7**:519.

YEANDLE, S. 1957. Studies on the slow potential and the effects of cations on the electrical responses of the *Limulus* ommatidium. Ph.D. Thesis. Johns Hopkins University. Baltimore, Md.

YEANDLE, S., and J. B. SPIEGLER. 1973. Light-evoked and spontaneous discrete waves in the ventral nerve photoreceptor of *Limulus*. *J. Gen. Physiol.* **61**:552.